Supporting Information

Efficient Electron Injection from Acyloin-Anchored Semi-Squarylium Dyes into Colloidal TiO_2 films for Organic Dye-Sensitized Solar Cells

Andreas F. Bartelt,[†,] Robert Schütz,[†] Christian Strothkämper,[†] Joachim Schaff,[†] Stephan Janzen,[†] Paja Reisch,[†] Ivo Kastl,[†] Manuel Ziwritsch,[†] Rainer Eichberger,[†] Gerda Fuhrmann,[‡,]*, David Danner,[‡] Lars-Peter Scheller,[‡] and Gabriele Nelles[‡]*

[†]Helmholtz-Center Berlin for Materials and Energy, Hahn-Meitner-Platz 1, 14109 Berlin, Germany

[‡]Materials Science Laboratory, Sony Deutschland GmbH, D-70327 Stuttgart, Germany

Andreas.Bartelt@helmholtz-berlin.de
gerda.fuhrmann@eu.sony.com

1. Photovoltaic performance

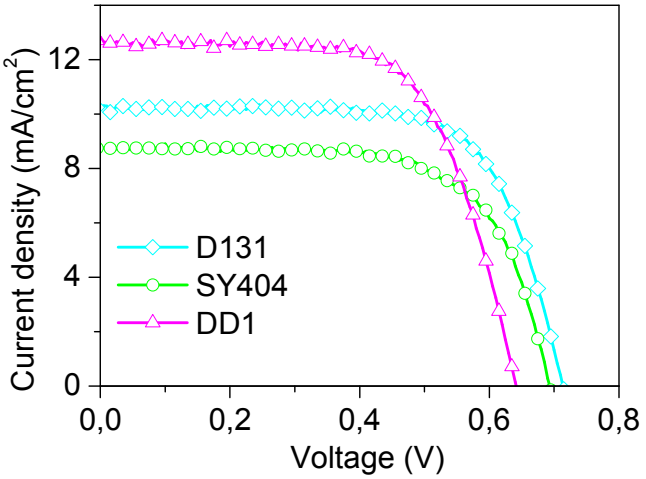

Figure S 1. *J-V* curves of DSCs based on **SY404**, **DD1** and **D131** recorded under following conditions: irradiated light: AM1.5G (100 mW/cm^2); photoelectrode: TiO_2 (5 µm transparent + 3 µm scattering layer), 0.188 cm^2; electrolyte: 1.4 M 1,2-dimethyl-3-propylimidazolium iodide / 0.15 M NaI / 0.075 M I_2 / 0.2 M *tert*-butylpyridine in methoxyacetonitrile.

2. **D131** blue shift

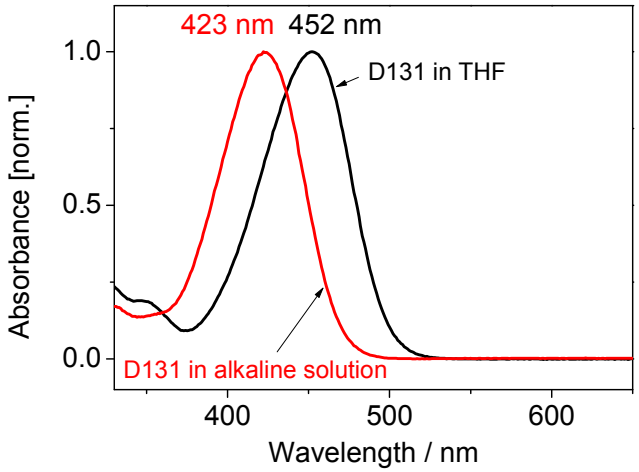

Figure S 2. The **D131** absorbance in THF was compared with the absorbance of **D131** dissolved in an alkaline solution based on a 1:1 mix of 1M tetrabutylammoniumhydroxide and methanol (concentration 3.33 *10^{-5} M). An almost 30 nm blue shift was found similar to the TiO_2-induced blue shift.

3. Coherent artifact of D131 transient absorption

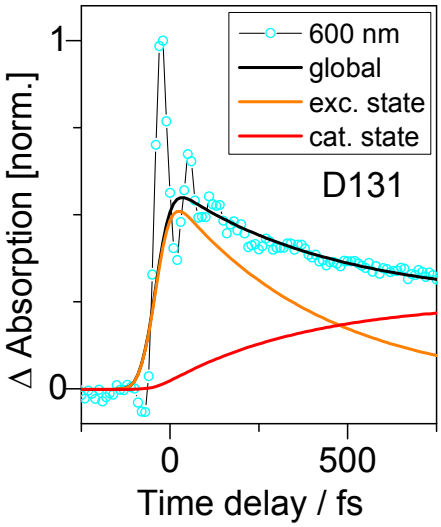

Figure S 3. TiO_2/**D131** transient absorption trace of the first few hundred femtoseconds including the fit results. The oscillatory structure of the signal around time zero is due to the temporal overlap of pump and probe pulses on the glass substrate ("coherent artifact"). The global fitting procedure allowed retrieving the signal dynamics underlying the coherent artifact.

4. Fitting procedure of the transient absorption data

Due to the mixing of excited and cationic states, the contributions from excited and cationic states were disentangled by taking advantage of the fact that the decay of the excited state N^* and the rise of the cationic state N^+ are coupled as the injection process occurs from the excited state. The transients were analyzed with a global fit using a model which describes the signal as the solution of a simple rate equation:

$$N \rightarrow N^* \rightarrow N^+ \rightarrow N$$

The simulated process can be described by coupled differential equations including a generation term $G(t)$ which entails the system response. Assuming no intermediate state, the coupling requires that the excited state decay rate is identical to the generation rate of the cationic state. This rate is called the injection rate r_{inj}. The temporal evolution of the excited state N^* can be expressed by:

$$\frac{dN^*}{dt} = G(t) - r_{inj} \cdot N^*$$

Accordingly the temporal evolution of the cationic state N^+ can be expressed as the depopulation of the excited state given by the injection rate r_{inj} and a depopulation of the cationic state given by the recombination rate r_{rec}:

$$\frac{dN^+}{dt} = r_{inj} \cdot N^* - r_{rec} \cdot N^+$$

Introducing a mixing coefficient α, the resulting single state signals can be superimposed to give the measured signal $N(t)$:

$$N(t) = A \cdot [\alpha \cdot N^* + [1 - \alpha] \cdot N^+]$$

Herein A is a scaling factor taking into account that different system response widths result in different $G(t)$ amplitudes while $N(t)$ is normalized to 1. Applying this model to the transients,

the injection time constants $\tau_{inj} \sim 1/r_{inj}$ could be derived using a least-square fit based on an iterative quasi-Newton algorithm with predefined boundaries. The differential equations included in this model were solved by a standard ODE-solver (ordinary differential equation). For this model it was assumed that the TA spectra probed the same electronic transitions regardless the different probe wavelengths for each dye. Only the excited and cationic state populations could vary. Thus, the global fitting procedure yielded one time constant per dye. The transient absorption spectra were concatenated and the sum of squares simultaneously reduced with regard to all transients using one global injection rate, but different mixing coefficients and scaling factors for each treated probe wavelength.

5. TiO_2 valence band onset

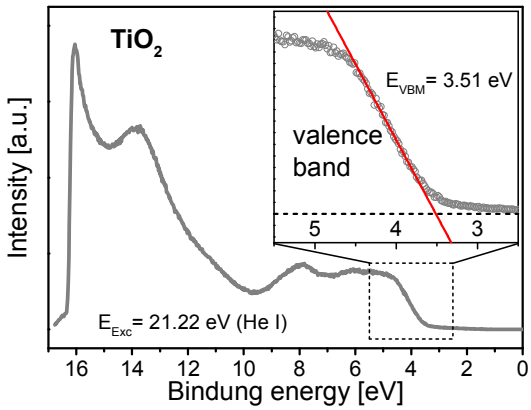

Figure S 4. UPS spectra of nc-TiO_2. The inset shows the onset of the TiO_2 valence band, and the intersection of a linear fit to this onset with the base line represents the binding energy of the valence band minimum of E_{VBM}=3.51 eV.

6. TiO_2 band gap

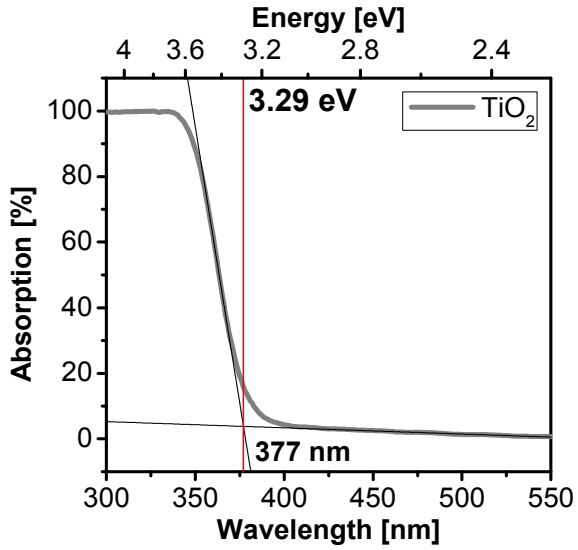

Figure S 5. Determination of the TiO_2 band gap from the extrapolated linear fit to the absorption onset. The intersection with the extrapolated baseline is a good estimate of the band gap.

7. Semi-squarylium dye synthesis and analytical data

The synthesis of the dyes **SY404** and **DD1** is illustrated in **Figure S 6**. The simple dye **SY404** was synthesized from commercially available materials following the method reported by Terpetschnig.[1] Firstly, a condensation of the N-propyl indolium heteroaromate **1** with one equivalent of 3,4-diethoxy-3-cyclobutene-1,2-dione **2** in the presence of triethylamine was carried out. By alkaline hydrolysis of the diethyl ester groups of **3** and subsequent protonation by treatment with aqueous hydrochloric acid the dye **SY404** was formed. The other dye **DD1** was synthesized by a similar method. In a prior step, firstly, the brominated heteroaromate **4** was prepared by the Fischer indole synthesis followed by a subsequent alkylation with hexyl iodide.[2] The longer alkyl chain was chosen because of the lower volatility of hexyl iodide compared to the propyl iodide allowing good control in the synthesis. With the longer alkyl chain, additionally, a better solubility of the products was provided. The following condensation reaction of **4** with **2** gave the brominated semi-squarylium **5**. The commercially available ethoxy functionalized triphenylaminethienyl boronic acid **6,** which was prepared in

a prior synthesis, was than introduced at the semi-squarylium core by a standard Suzuki coupling to yield the dye **DD1**. Under basic conditions during the coupling reaction simultaneous hydrolysis of the diethyl ester groups of the squaric acid moieties took place.

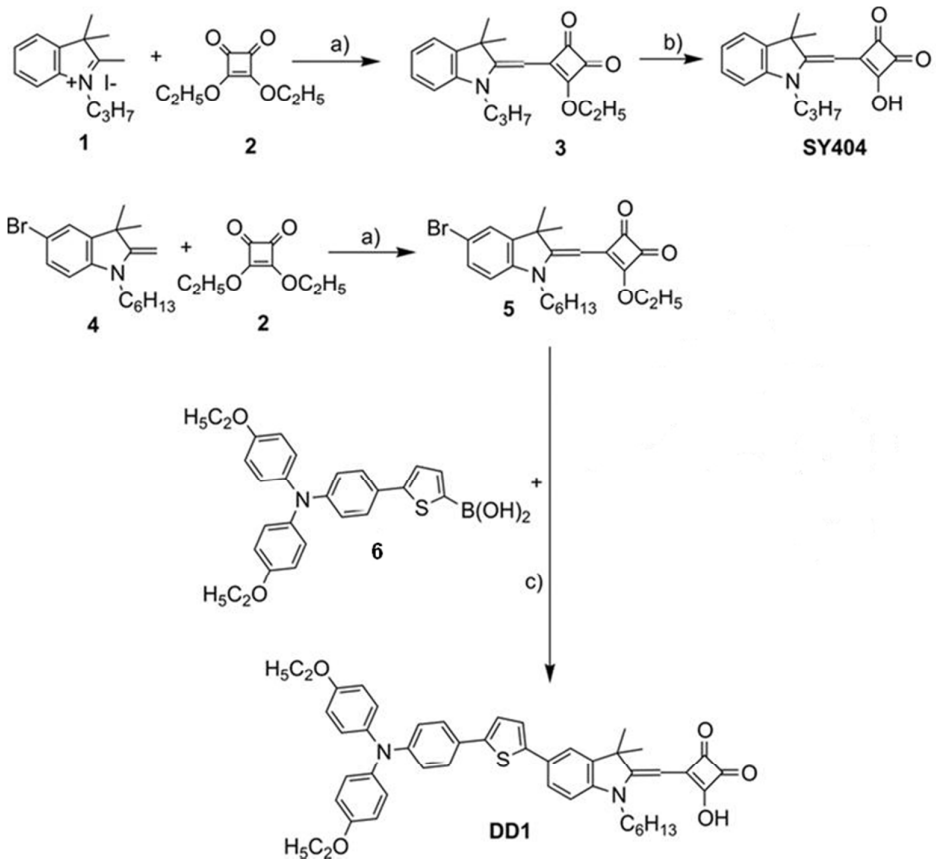

Figure S 6. Synthesis scheme of semi-squarylium dyes: a) ethanol, triethylamine, 65°C, 12 h; b) ethanol, 2M aq. NaOH, 3 h, RT; c) toluene/ MeOH (1/1), K_2CO_3, $Pd(PPh_3)_4$, 130°C, 12h; d) toluene/ MeOH (1/1), K_2CO_3, $Pd(PPh_3)_4$, 130°C, 12h.

The semi-squarylium dyes are stable yellow to orange-red microcrystalline solids with good solubility in conventional polar organic solvents. Their chemical structures were fully characterized with ^{1}H NMR, ^{13}C NMR and HRMS. They and their corresponding precursors exhibited characteristic signals in ^{1}H- and ^{13}C-NMR spectra which could be attributed to the substituents at their heterocyclic moieties. In the NMR spectra of the closest precursors **3** and **5**, the detected signals could be assigned to the diethyl ester moieties. In DMSO-d_6 the OH

proton signals of the squaric acid moiety of **SY404** and **DD1** could not be detected unambiguously due to the presence of traces of water in the solvent. Only when we employed THF-d_8, trace signals attributable to the proton of OH moiety at 10.89 ppm, 10.91 ppm and 10.95 ppm respectively, were detected.

SY404: mp 228.1 °C; ^{1}H-NMR (400 MHz, DMSO-d_6, δ): 7.23 (d, ^3J(H,H)=7.32 Hz, 1H; Ar H), 7.13 (dt, ^3J(H,H)=7.67 Hz, ^4J(H,H)=1.11 Hz, 1H; Ar H), 6.85 (d, ^3J(H,H)= 7.90 Hz, 1H; Ar H), 6.82 (t, ^3J(H,H)=7.35 Hz, 1H; CH_{arom}), 5.38 (s, 1H; C=CH), 3.67 (t, ^3J(H,H)=7.30 Hz, 2H; N-CH_2), 1.63 (m, 2H; CH_2), 1.48 (s, 6H; CH_3), 0.92 (t, ^3J(H,H)=7.40 Hz, 3H; CH_3); ^{13}C-NMR (100 MHz, DMSO-d_6, δ): =209.74, 195.10, 178.74, 157.64, 144.09, 139.75, 127.21, 121.51, 119.41, 106.72, 84.10, 45.74, 42.90, 27.57, 19.07, 11.23; HRMS (ESI, m/z) calcd. for $C_{18}H_{19}NO_3$ 297.35; found 297.43.

DD1: mp 165°C; ^{1}H-NMR (400 MHz, DMSO-d_6, δ): 7.47 (d, ^4J(H,H)=1.68 Hz, 1H; Ar H), 7.42 (m, 3H; Ar H), 7.18 (m, 2H; Ar H), 7.01 (m, 4H; Ar H), 6.83 (m, 7H; Ar H), 5.70 (s, 1H; C=CH) 3.98 (q, ^3J(H,H)=6.97 Hz, 4H; CH_2), 3.79 (m, 2H; CH_2), 1.68 (s, 6H; CH_3), 1.50-1.25 (m, 12H; CH_2, CH_3), 0.88 (t, ^3J(H,H)=7.07 Hz, 3H; CH_3); ^{13}C-NMR (100 MHz, DMSO-d_6, δ): =210.12, 195.08, 178.30, 156.92, 155.08, 147.63, 143.67, 142.17, 140.88, 140.70, 139.63, 126.69, 125.79, 125.53, 125.45, 124.59, 122.98, 122.83, 119.36, 118.59, 106.94, 84.85, 63.12, 45.71, 30.98, 27.50, 25.98, 25.68, 21.99, 14.67, 13.80; HRMS (ESI, m/z): calcd. for $C_{47}H_{48}N_2O_5S$ 752.96; found 751.20 [M^+-H].

REFERENCES

(1) Terpetschnig, E.; Lakowicz, J. R. Synthesis and Characterization of Unsymmetrical Squaraines: A New Class of Cyanine Dyes. *Dyes Pigments* **1993**, *21*, 227–234.

(2) Fischer, E.; Jourdan, F. Ueber Die Hydrazine Der Brenztraubensäure. *Berichte Dtsch. Chem. Ges.* **1883**, *16*, 2241–2245.